Effect of anti-site disorder on magnetism in La_2NiMnO_6

Somnath Pal,[1] Sharada Govinda,[1] Manik Goyal,[1] Soham Mukherjee,[1] Banabir Pal,[1] Rana Saha,[2] A. Sundaresan,[2] Somnath Jana,[3] Olof Karis,[3] John W. Freeland,[4] and D. D. Sarma[1,*]

[1]*Solid State and Structural Chemistry Unit, Indian Institute of Science, Bengaluru 560012, India*

[2]*Chemistry and Physics of Materials Unit, Jawaharlal Nehru Centre for Advanced Scientific Research, Jakkur, Bengaluru 560064, India*

[3]*Molecular and Condensed Matter Physics, Department of Physics and Astronomy, Uppsala University, Box 516, 75120 Uppsala, Sweden*

[4]*Argonne National Laboratory, Argonne, Illinois 60439, USA*

(Received 13 July 2017; revised manuscript received 9 November 2017; published 25 April 2018; corrected 18 June 2018)

La_2NiMnO_6 has been reported to exhibit a paramagnetic to ferromagnetic transition with a transition temperature of ∼260 K. However, most of its magnetic properties, such as the saturation magnetization and even the transition temperature, appear to vary considerably among different reports. This is possibly because the crystallographic structure as well as the extent of the anti-site disorder (ASD) at the Ni/Mn sites are strongly influenced by the choice of synthesis routes. There are diverse reports connecting the extent of ASD to the valencies of Ni and Mn ions, such as Ni^{2+}-Mn^{4+} and Ni^{3+}-Mn^{3+}, including suggestions of thermally induced valence transitions. Consequently, these reports arrive at very different conclusions on the mechanism behind the magnetic properties of La_2NiMnO_6. To address the correlation between ASD and valency, we have carried out a comparative study of two monoclinic La_2NiMnO_6 polycrystals with different degrees of ASD. Using a combination of x-ray absorption spectroscopy, x-ray magnetic circular dichroism, and magnetometry, we conclude that the valency of the transition metal ions, and the transition temperature, are insensitive to the extent of ASD. However, we find the magnetic moment decreases strongly with an increasing ASD. We attribute this effect to the introduction of antiferromagnetic interactions in the anti-site disordered regions.

DOI: 10.1103/PhysRevB.97.165137

I. INTRODUCTION

La_2NiMnO_6 is a ferromagnetic insulating double perovskite that has been widely investigated over the last decade [1–11]. La_2NiMnO_6 can form in two distinct crystallographic forms, a monoclinic $P2_1/n$ structure or in a rhombohedral $R\bar{3}$ structure. The unusual behavior in magnetic and dielectric properties of this material in nano, thin film, single crystal, and polycrystalline phases has attracted attention from many different groups [8,12–19]. It is found that the dielectric, magnetic, and the magnetoresistance properties of these compounds are closely coupled. The origin of unusual magnetic and magnetoelectric behavior have been extensively discussed in the literature, and there are many conflicting experimental results with widely varying explanations. As an example of the discrepancies found, we note that the field cooled (FC) and zero field cooled (ZFC) magnetic properties of La_2NiMnO_6 as a function of temperature differs significantly between different reports [16,20–23]. These specific differences most likely arise from different synthesis conditions used in these different works. Furthermore, conflicting points of view have been reported in the literature regarding the valence state of the magnetic ions, Mn and Ni, and the origin of a magnetically ordered state. A ferromagnetic transition with a Curie temperature T_C of 280 K was first reported and explained to be due to Ni^{3+}-O^{2-}-Mn^{3+} superexchange interactions by Goodenough *et al.* [24]. Later, Blasse *et al.* [25] suggested that the superexchange interaction in Ni^{2+}-O^{2-}-Mn^{4+} causes the ferromagnetic ordering. Since then, there are many reports of favoring one or the other mechanism [15,20,21,23,26,27]. Though the valence states of the magnetic cations and the origin of magnetism have been discussed in many reports, the valency of Ni and Mn was only recently clarified in an x-ray absorption spectroscopy (XAS) study by Choudhury *et al.* [8].

The origin of ferromagnetism has also been investigated with the help of 55Mn NMR [28,29], neutron diffraction studies [30], and first-principle calculations [8,31]. In Ref. [31] it was furthermore concluded that the origin of ferromagnetism in La_2NiMnO_6 is superexchange mediated through the Ni^{2+}-O^{2-}-Mn^{4+} interaction. There are also reports about two ferromagnetic transitions in a single system [23,27]—one at a higher temperature (T_C ∼ 266 K) and another at a lower temperature (∼100 K). The latter was attributed to inhomogeneities in the sample with two phases (Ni^{2+}-Mn^{4+} and Ni^{3+}-Mn^{3+}) having distinctly different electronic properties [15,20,23,27].

In Ref. [8] the low temperature magnetic transition was identified to be glassy due to the presence of anti-site disorder (ASD) in the system. ASD leads to Ni^{2+}-O^{2-}-Ni^{2+} and Mn^{4+}-O^{2-}-Mn^{4+} antiferromagnetic interactions resulting in magnetic frustration. Large magnetodielectric coupling [1,8] was also observed near room temperature in La_2NiMnO_6 and was attributed to Ni^{2+} and Mn^{4+} cation ordering.

Based on the above mentioned literature, it becomes evident that ASD plays a major role in the magnetic, dielectric, and magnetodielectric properties. Thus, the understanding of

*Also at Jawaharlal Nehru Centre for Advanced Scientific Research, Bengaluru; sarma@iisc.ac.in

 ©2018 American Physical Society

ASD and the nature of magnetic interactions in ASD phase is important. The ASD has been suggested to give rise to antiferromagnetic interactions [8], but there is no conclusive experimental verification so far. Ordered and disordered La_2NiMnO_6 thin films were studied by Singh *et al.*, but their disordered sample exhibited a strongly lowered T_C compared to other studies [23]. The present study is aimed at eliminating all uncertainties regarding the role of ASD and valency of magnetic cations. This has been achieved by XAS, XMCD, and magnetometery experiments performed on two monoclinic La_2NiMnO_6 samples, but with a large difference in ASD.

II. EXPERIMENTAL METHOD

La_2NiMnO_6 has been synthesized in its pure monoclinic phase using a sol-gel method, similar to Ref. [27]. Stoichiometric amount of La_2O_3, $Ni(NO_3)_2 \cdot 6H_2O$, and $MnCO_3$ were dissolved in dilute nitric acid. Due to the hygroscopic nature of the rare earth oxide La_2O_3, it was preheated at 900 °C for 12 h to remove moisture from the precursor. Ethylene glycol and citric acid were added to the solution for chelation and gel formation, which ensured the completion of the reaction. The resulting solution was then heated at 170 °C to evaporate the solvents completely, giving a dark brown powder, which was subsequently heated at 450 °C for 6 h. The obtained powder was again heated at 1350 °C in a flow of argon for 6 h. Two different approaches were followed to cool the sample from this highest temperature in order to influence the extent of ordering between Mn and Ni sites by kinetically controlling the Mn/Ni ASD formation. In one case, the temperature of the sample was brought down in a controlled manner with a slow cooling rate of 1 °C/min. For the other sample, the furnace power supply was switched off to initiate rapid cooling; average cooling rates in this case were ∼14 °C/min down to 1000 °C, 6 °C/min till 700 °C, and 3 °C/min till 300 °C. Our intention was to achieve a highly ordered sample with a slow cooling protocol and a considerably disordered sample with a rapid cooling. It is curious to note that exactly the opposite was achieved in reality, with the first sample being disordered and the second ordered, as shall be shown later in the Result section.

Crystal structure of the two La_2NiMnO_6 samples were determined using powder x-ray diffraction (XRD) measurements with a Panalytical Philips diffractometer using Cu-K_α radiation ($\lambda = 1.54056$ Å). Rietveld refinements were performed to estimate structural parameters using the FULLPROF suite [32]. Field cooled (FC) and zero field cooled (ZFC) dc magnetization measurements were performed in the temperature range of 10 to 350 K in an applied field of 100 Oe using a Quantum Design SQUID magnetometer.

In order to characterize the valency of the transition metal cations, XAS measurements at the La $M_{4,5}$, Ni $L_{2,3}$, and Mn $L_{2,3}$ edges were performed at the I1011 beamline at MAX-lab, Sweden [33]. X-ray absorption spectra were recorded in the total electron yield (TEY) mode by recording the sample drain current as a function of the photon energy. The base pressure of the chamber was maintained at around 7×10^{-9} mbar. Sample surfaces were prepared by *in situ* scraping of the samples with a diamond file prior to the XAS measurement. X-ray magnetic circular dichroism (XMCD) spectra were recorded at the 4-ID-C beamline, Advanced Photon Source (APS), ANL, USA. Each spectrum was simultaneously recorded in the more surface sensitive TEY mode and the more bulk-sensitive total fluorescence yield (TFY) mode, while applying a 5 kOe magnetic field and at a temperature of 150 K. All spectra were normalized by the photon flux.

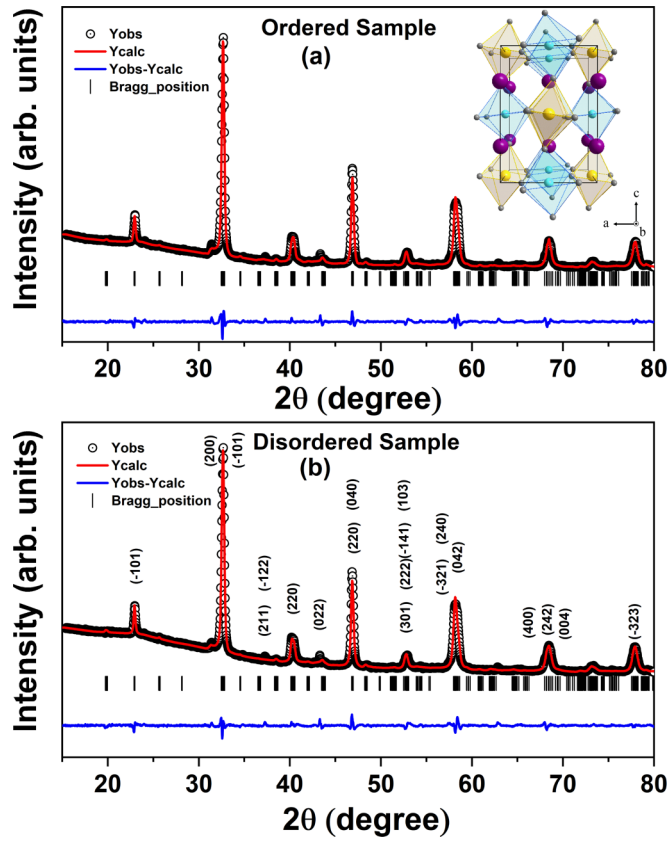

FIG. 1. Powder x-ray diffraction data with the corresponding Rietveld refinement and residual of experiment − fit of (a) ordered La_2NiMnO_6 and (b) disordered La_2NiMnO_6. (See text.) Inset of (a) presents a schematic of the distribution of La (purple), Mn (cyan), Ni (yellow), and O (gray) atoms within the unit cell of monoclinic La_2NiMnO_6.

III. RESULTS AND DISCUSSIONS

In Figs. 1(a) and 1(b) we show the recorded powder XRD data, together with the Rietveld refinement results, of the ordered and disordered samples, respectively. These results confirm the formation of both samples purely in monoclinic ($P2_1/n$) phase without any rhombohedral ($R\bar{3}$) phase as an impurity. The inset of Fig. 1(a) exhibits a schematic illustration of monoclinic La_2NiMnO_6 [27]. Ni and Mn are octahedrally coordinated with six oxygen atoms. The NiO_6 and MnO_6 corner-shared octahedra appear alternately in the fully ordered unit cell, representing two sublattices: anti-site disorder represents a point defect with a Mn ion occupying a Ni site or vice versa. In absence of any vacancies, anti-site disorder appears necessarily in pairs due to the interchange of positions of a pair of Ni and Mn ions. The Ni-Mn ordering related peak is expected to appear at $2\theta \approx 20°$ (see Fig. 1) with an intensity of

TABLE I. Lattice parameters for ordered and disordered La_2NiMnO_6 samples derived from the Rietveld refinement. Standard deviations are indicated within parentheses.

Sample	Unit cell parameters					
	a (Å)	b (Å)	c (Å)	$\alpha = \gamma$ (deg)	β (deg)	Cell volume (V) (Å^3)
Ordered	5.4636(5)	5.5120(4)	7.7550(3)	90	90.288(4)	233.5115
Disordered	5.4615(5)	5.5119(4)	7.7512(3)	90	90.233(5)	233.3333

0.6% of the most intense peak at ∼32°; this makes this feature masked by the background signal. Moreover, the maximum change expected in this extremely weak order-related signal is only about 17% between a fully ordered and completely disordered structures due to very similar scattering cross sections of x rays by Mn and Ni ions. The expected change in this weak peak for the two samples, based on estimates of the extents of ASD from the saturation magnetizations, discussed later, is only about 7%. These considerations explain why Rietveld analysis is not sufficiently sensitive to probe the extent of such ASD in this system and consequently, has not been used for this purpose. The cell parameters obtained from the Rietveld analysis are given in Table I, indicating no significant variation in the structure.

Choudhury *et al.* recently showed that the valence states of Ni and Mn in a particular sample of La_2NiMnO_6 are Ni^{2+} and Mn^{4+}, respectively [8]; however, any possible impact of a changing level of disorder on the valence states of these ions was not investigated in this earlier report. This is particularly significant in view of claim of correlation between valence state and the extent of disorder in the reported literature. Among the measurement techniques available for determining the valence state of a particular species, XAS is a very sensitive and direct method for this purpose. In soft x-ray absorption spectroscopy, the transition from $2p^6 3d^n$ initial state to $2p^5 3d^{n+1}$ configuration in the final state provides an extremely sensitive local probe, ideal to study the valence [34], and spin [35,36] character in initial states and crystal field environment of the system.

Figures 2(a) and 2(b) display the normalized Mn $L_{2,3}$ XAS spectra measured in TEY and TFY, respectively. Standard Mn $L_{2,3}$ XAS for +2, +3, and +4 valency are shown in Fig. 2(c). Ignoring slight differences in the background signals arising from the two compounds with vastly different extent of ordering, the Mn $L_{2,3}$ XAS spectra of the ordered and disordered La_2NiMnO_6 do not differ either in TEY or the TFY mode. Comparing with the spectral features of standard compounds, shown in Fig. 2(c), we find that the spectral features from both samples match quite well with that of Mn^{4+} in $LiNi_{0.5}Mn_{0.5}O_2$ compared to Mn^{3+} in $LaMnO_3$ and Mn^{2+} in MnO; this is made further evident by the comparison of Mn^{4+} spectral features from $LiNi_{0.5}Mn_{0.5}O_2$ reproduced in Fig. 2(a) for a direct comparison with those of ordered and disordered La_2NiMnO_6. It is to be noted that spectral features of Mn^{4+} species in $LiNi_{0.5}Mn_{0.5}O_2$ are quite similar to reports of spectral features of Mn^{4+} species in other related oxide systems, such as MnO_2 and $SrMnO_4$ [37]. These comparisons suggest that Mn is in +4 valence state in both samples. Furthermore, very similar Mn $L_{2,3}$ peak positions in both the TEY and TFY spectra reveal that the valence state of Mn does not differ at the near-surface region compared to the bulk. The difference in the relative intensity for the L_3 and L_2 peaks in TFY spectra relative to the TEY spectra, with L_2 intensities considerably enhanced for the TFY mode, are due to self-absorption and saturation effects [38].

The Ni $L_{2,3}$ edge XAS spectra in TEY and TFY are shown in Figs. 3(a) and 3(b), respectively. The Ni L_3 edge is overlapped with the intense La M_5 edge, which obscures the Ni spectral features. Therefore, we rely on the spectral features at L_2 [magnified in the inset of Fig. 3(a)] for our analysis. For the TFY mode, self-absorption effects favor intensities of higher energy features relative to lower energy spectral features,

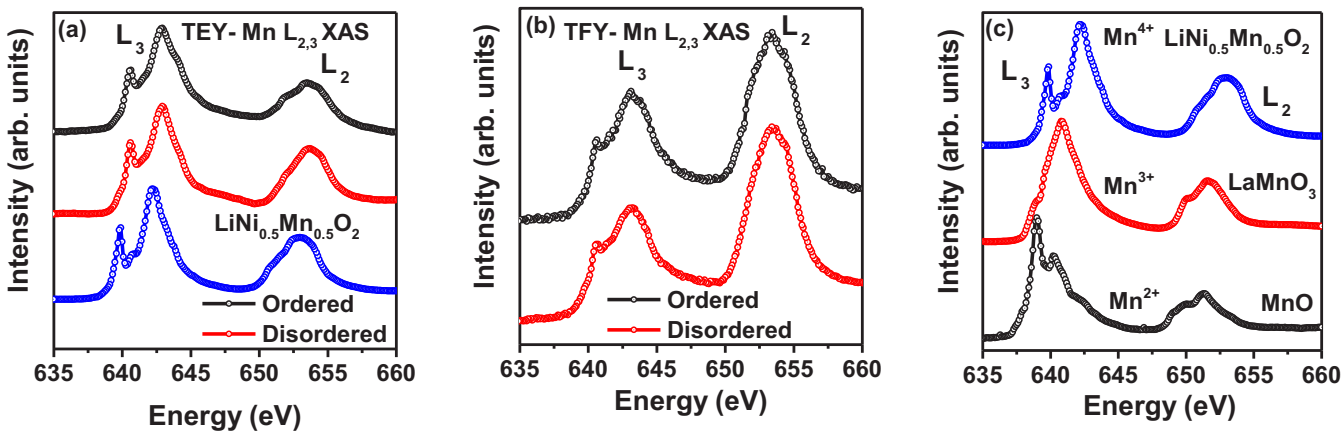

FIG. 2. XAS of Mn $L_{2,3}$ edge of ordered and disordered La_2NiMnO_6 recorded in the TEY (a) and TFY (b) modes. (a) Also includes the spectrum of $LiNi_{0.5}Mn_{0.5}O_2$ to illustrate a typical XAS of Mn^{4+} species in TEY mode. (c) XAS spectra of a few standard Mn-oxides samples, obtained in the TEY mode, to illustrate the distinctive spectral features of Mn^{2+}, Mn^{3+}, and Mn^{4+} species.

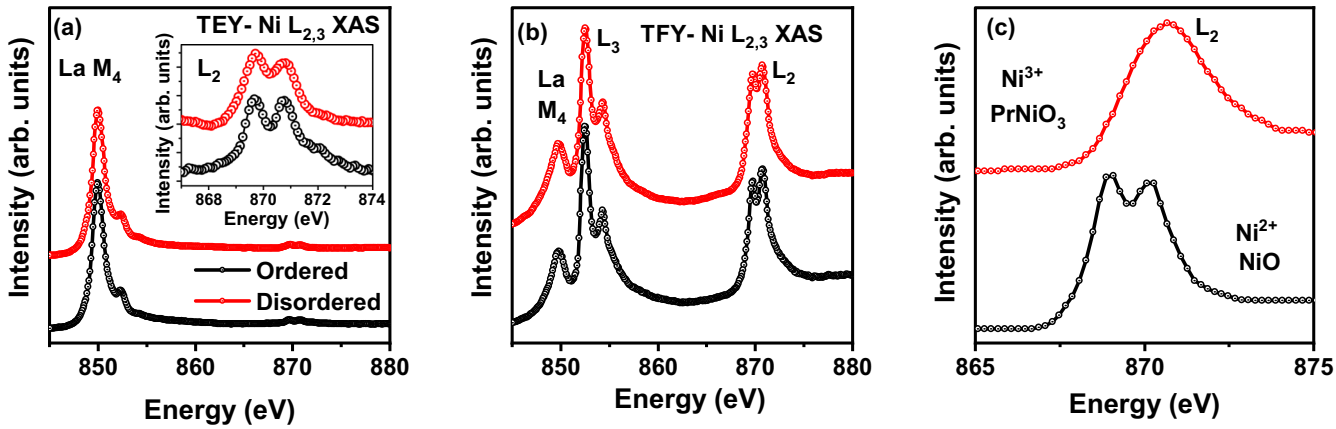

FIG. 3. XAS of Ni $L_{2,3}$ edge of ordered and disordered La_2NiMnO_6 recorded in the TEY (a) and TFY (b) modes. (c) XAS of NiO and $PrNiO_3$, illustrating characteristic spectral features of Ni^{2+} and Ni^{3+} states, respectively.

making Ni L_2 spectral features more clearly visible, as shown in the main frame of Fig. 3(b). Figure 3(c) shows $L_{2,3}$ XAS spectra of Ni^{2+} in NiO and Ni^{3+} in $PrNiO_3$ [8]. Line shapes of Ni L_2 edge in Figs. 3(a) and 3(b) are very similar to that of NiO shown in Fig. 3(c). Therefore, we argue from the Ni $L_{2,3}$ XAS spectra that the oxidation states of Ni ions are +2 in both samples, which is consistent with the observation of the Mn^{4+} state from the Mn $L_{2,3}$ XAS spectra. X-ray absorption spectroscopy thus establishes a constant valency for the Ni and Mn ions independent of the extent of disorder in the samples.

While the valence states at individual atomic Ni and Mn sites, and consequently the gross electronic properties of La_2NiMnO_6, appear to be insensitive to the extent of ASD present in these samples, we next show that magnetic properties are profoundly affected by the extent of this disorder and provide a microscopic understanding of the same, based on a combination of dc magnetic and XMCD measurements. Figure 4 shows results of magnetization M as a function of applied field H at 2 K for the ordered and disordered La_2NiMnO_6 samples. With enhanced disorder, a large decrease

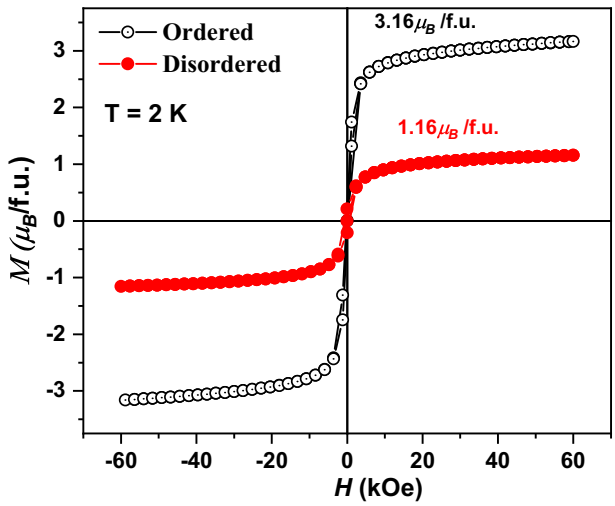

FIG. 4. M vs H data of ordered (black open circle) and disordered (red closed circle) La_2NiMnO_6 at $T = 2$ K.

in the saturation magnetization can be clearly observed in the plot. The saturation magnetic moment for a perfectly ordered structure should be 5 μ_B/f.u., since Ni^{2+} and Mn^{4+} contribute two and three unpaired electrons, respectively, the two atomic sites being ferromagnetically coupled arising from the ferromagnetic superexchange interaction between Ni^{2+} d^8 and Mn^{4+} d^3 configurations via fully filled oxygen $2p$ orbitals in octahedral symmetries [31]. A saturation moment of 3.2 μ_B/f.u. for the present "Ordered" sample suggests a more ordered state than reported in Ref. [8] with a saturation moment of 3.0 μ_B/f.u. The impact of an ASD on the magnetic moment can be understood easily by assuming the interchange of one Ni^{2+} with one Mn^{4+}. In the ideally ordered case, each Ni^{2+} ion is surrounded by six Mn^{4+} ions, coupled ferromagnetically; likewise, each Mn^{4+} ion is coupled ferromagnetically to six Ni^{2+} ions surrounding it. If a nearest Ni^{2+}-Mn^{4+} pair forms the ASD by interchanging positions of the two ions, we obtain around the defect Ni^{2+} site five Ni^{2+} and one Mn^{4+} and *vice versa* for the Mn^{4+} defect site with five Mn^{4+} and one Ni^{2+}. The antiferromagnetic superexchange for Ni^{2+}-O^{2-}-Ni^{2+} and Mn^{4+}-O^{2-}-Mn^{4+} dominate these local defect sites, forcing the Ni^{2+} and Mn^{4+} involved in forming the ASD to be antiferromagnetically oriented with respect to the remaining ferromagnetically coupled lattice. Thus, each ASD converts a pair of Ni^{2+} and Mn^{4+} ions with a total moment of 5 μ_B coupled ferromagnetically with the rest of the system into a pair carrying the same 5 μ_B, but coupled antiferromagnetically, thereby reducing the magnetic moment of the sample by 10 μ_B for each ASD pair. Thus, a net magnetic moment of 3.2 μ_B/f.u., with a reduction of 1.8 μ_B/f.u. from the fully ordered moment of 5 μ_B/f.u., indicates the presence of ~18% ASD. Similarly, the moment obtained for the disordered sample, 1.2 μ_B/f.u., suggests a 38% ASD in this case. Noting that the maximum extent of ASD in this definition is 50% that leads to a zero net moment case, a 38% disorder indicates a very high degree of disorder in this sample; in contrast, the ordered sample exhibits a fairly high degree of ordering (~18% disorder).

The dc magnetic susceptibility measurements at a field of 100 Oe and the inverse susceptibilities derived from these are shown in Figs. 5(a)–5(d) for both samples. The ferromagnetic transition temperature ($T_C \sim 266$ K) remains unchanged for

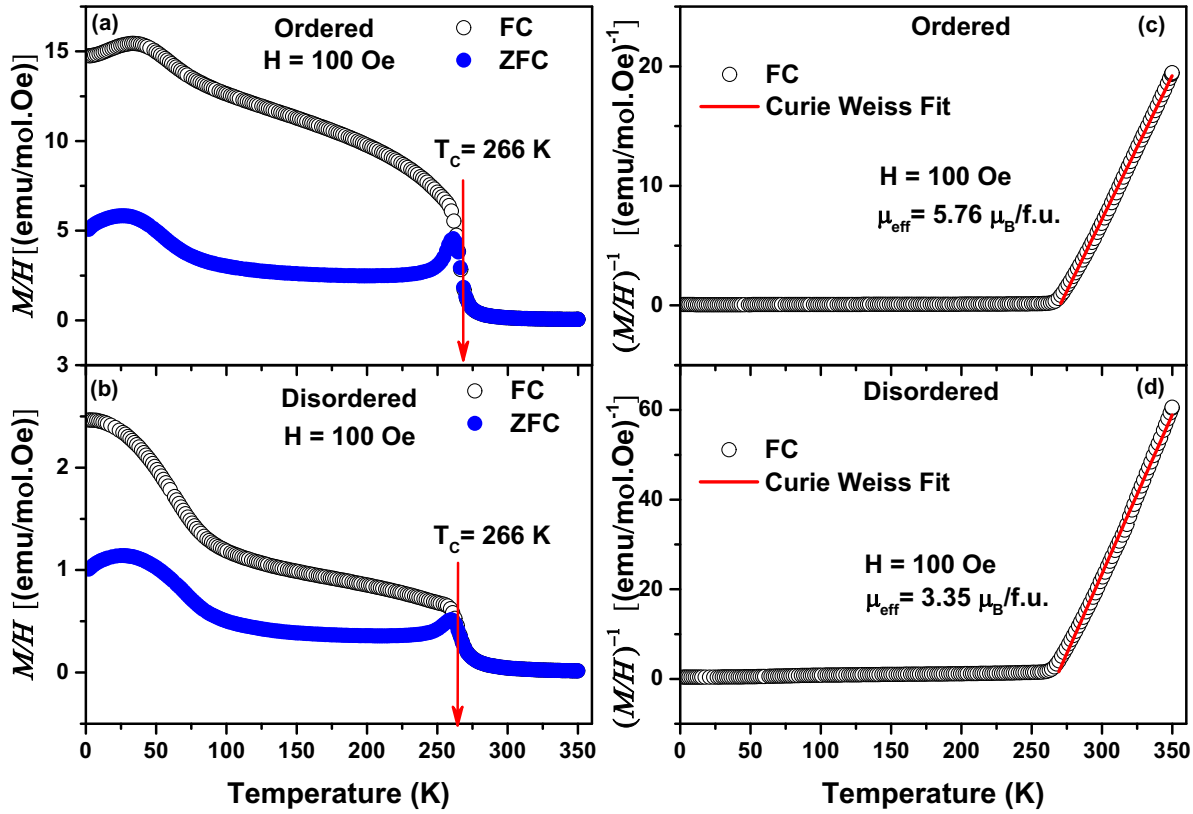

FIG. 5. (a) and (b) dc magnetic FC and ZFC measurements at a field of 100 Oe and their inverse susceptibilities (c) and (d) for ordered and disordered samples of La_2NiMnO_6, respectively.

both samples, suggesting that the strength of the primary interaction, responsible for the long-range magnetic ordering, is insensitive to the extent of disorder. This is in accordance with the finding that the XAS measurements indicate that both samples contain Mn^{4+} and Ni^{2+} ions only, but is in contrast to most of the previous reports on this system [15,20,23,27]. This is strongly reminiscent of the case of Sr_2FeMoO_6, where also it has been shown [39] that samples with a very high degree of disorder exhibit magnetic transition temperatures almost identical to those of highly ordered samples, though the saturation magnetization can differ by as much as a factor of 4. The anomaly present at low temperatures (below 150 K) in both samples has been attributed to spin glass type behavior [8].

In the paramagnetic region, the magnetic susceptibility of the sample exhibits a Curie-Weiss behavior with the paramagnetic susceptibility ($\chi = \frac{M}{H}$) given by

$$\chi = \frac{C}{T - \theta}, \tag{1}$$

where C is the Curie constant, and θ is the Curie-Weiss temperature. The Curie constant C in the above equation is related to effective paramagnetic moment μ_{eff} by

$$\mu_{\text{eff}} = \sqrt{\frac{3k_B C}{N\mu_B^2}} = 2.827\sqrt{C}, \tag{2}$$

where k_B is the Boltzmann constant, μ_B is Bohr magneton, and N is the number of magnetic atoms per unit volume [1,40,41]. The inverse susceptibility, being proportional to (T-θ), appears as a straight line, when plotted as a function of the temperature, as shown in Figs. 5(c) and 5(d) The obtained Curie-Weiss temperature (θ), Curie constant (C), and effective magnetic moment (μ_{eff}), extracted from these data, via a least-squared-error fitting approach, are given in Table II for both compounds. As expected for a ferromagnet, we find positive Curie-Weiss temperature (θ) values for both ordered and disordered La_2NiMnO_6 samples. Almost identical values of θ for the two samples suggest that the ferromagnetic interaction, between Ni^{2+} and Mn^{4+} sites, or in other words, the superexchange interaction between these sites is not affected by the presence of even extensive disorder, though evidently there is a strong reduction in the effective paramagnetic moment with

TABLE II. Parameters calculated from Curie-Weiss fitting of ordered and disordered La_2NiMnO_6.

Sample	Curie-Weiss temperature (θ) (K)	Curie constant (C) (emu K mol^{-1} Oe^{-1})	μ_{eff} (μ_B/f.u.)
Ordered	270	4.16	5.76
Disordered	267	1.41	3.35

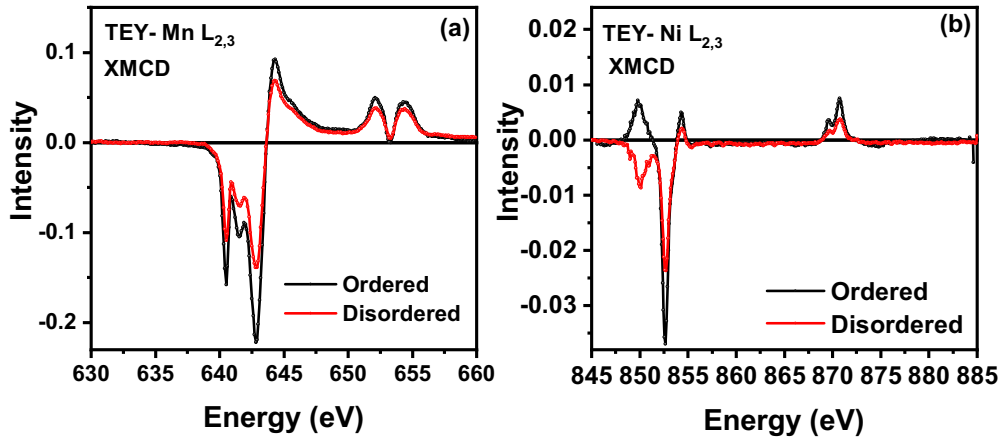

FIG. 6. (a) Mn $L_{2,3}$ edge XMCD spectra and (b) Ni $L_{2,3}$ XMCD spectra for both ordered and disordered La_2NiMnO_6 samples at TEY mode with an applied magnetic field 50 kOe at $T = 150$ K.

an increasing disorder. Specifically, the ordered La_2NiMnO_6 sample has an effective paramagnetic moment (μ_{eff}) of 5.8 μ_B/f.u., while for the disordered sample, it is only 3.4 μ_B/f.u. The lowering of μ_{eff} in the disordered sample indicates that increased ASD leads to increased antiferromagnetic interactions, in the form of strongly coupled Ni^{2+}-O^{2-}-Ni^{2+} and Mn^{4+}-O^{2-}-Mn^{4+} arrangements.

The XAS data discussed above already establishes that the Mn and Ni valencies do not change with disorder, thereby providing a basis to understand the constancy of θ and the magnetic ordering temperature T_C, but those results do not provide any insight into why the effective paramagnetic moment (Table II) and the saturation magnetization (Fig. 4) drop so significantly with increasing disorder. We have already suggested that this reduction in the magnetic moment with an increasing ASD density most likely arises from the antiparallel orientation of the pair of Ni^{2+} and Mn^{4+} ions involved in this defect formation with respect to the ferromagnetically coupled magnetic moment of the ordered lattice, leading to a reduction of 10 μ_B for each ASD pair formed. This would imply a simultaneous reduction of the average magnetic moments of both Mn^{4+} and Ni^{2+} sublattices to the total moment, which is measured by the saturation magnetization (Fig. 4).

To address this question, the element specific magnetic measurement XMCD was performed. The measured XMCD at the Mn and Ni $L_{2,3}$ edges in the TEY mode, relatively less influenced by self-absorption effects, was measured at 150 K in a magnetic field of 50 kOe, as shown for both samples in Figs. 6(a) and 6(b), respectively. The small, leading peak around 850 eV in the Ni L_3 edge XMCD Fig. 6(b) is an artifact arising from incomplete substraction of the signal arising from nonmagnetic La. The polarity of the XMCD signal at both Ni and Mn $L_{2,3}$ edges has the same sign for both samples. This means the majority of the Ni^{2+} and Mn^{4+} spin moments are aligned parallel for both samples. This result is consistent with the ferromagnetic behavior of La_2NiMnO_6 in both samples [42–44]. It is seen that the intensity of both Mn and Ni XMCD signals for the ordered sample is larger than those of the disordered La_2NiMnO_6 sample, which corroborates the results from dc magnetic measurements.

It is known that the XMCD signal can be quantitatively analyzed using well-known sum rules [45] to provide estimates of site-specific magnetic moments. While such an analysis of results in Fig. 6(a) indicate an average contribution of 1.3 and 0.4 μ_B per Mn^{4+} ion for the ordered and the disordered samples, respectively, a similar analysis for the Ni^{2+} signal in Fig. 6(b) is not possible due to the overlapping La M_4 signal (see Fig. 3). However, it is still possible to relate the extracted site-specific average magnetization of the Mn^{4+} sublattice from the XMCD results to the bulk magnetizations by noting that the total magnetization in these samples is contributed only by the Mn^{4+} ($3d^3$) and Ni^{2+} ($3d^8$) sites in the proportion of 3:2, with La^{3+} and O^{2-} being nonmagnetic. Thus, three-fifths of the total magnetization arises from Mn^{4+} and two-fifths from Ni^{2+}. Reference [45] showed that the saturation magnetization of La_2NiMnO_6 at 150 K is about 67% of its low temperature value. The low temperature saturation magnetization of the two samples here are 3.16 and 1.16 μ_B/f.u., shown in Fig. 4. This suggests that the saturation magnetization of our samples, if measured at 150 K, would be 2.1 and 0.8 μ_B/f.u. Three-fifths of these values, ~1.3 and 0.5 μ_B, that is the contribution of Mn^{4+} to the total bulk magnetizations, are in good agreement with XMCD estimates of 1.3 and 0.4 μ_B/Mn^{4+} for ordered and disordered samples at 150 K, respectively. These observations lend support to our suggestion above that the ASD leads to antiferromagnetic interactions in Mn^{4+}-O^{2-}-Mn^{4+} and Ni^{2+}-O^{2-}-Ni^{2+} bonds.

IV. CONCLUSION

In conclusion, we have synthesized two La_2NiMnO_6 samples in the monoclinic ($P2_1/n$) phase with strongly differing extents of anti-site disorder. Using x-ray absorption spectroscopy we have verified that the oxidation state of Ni is +2 and Mn is +4, independent of the amount of anti-site disorder. Our samples show ferromagnetic transition at ~266 K due to Ni^{2+}-O^{2-}-Mn^{4+} superexchange interaction, also independent of the amount of anti-site disorder. XMCD measurements show similar extents of reduction in the average Ni and Mn moments with an increasing disorder, providing evidence that anti-site disorder leads to the introduction of antiferromagnetic interaction through Ni^{2+}-O^{2-}-Ni^{2+} and Mn^{4+}-O^{2-}-Mn^{4+} superexchange.

ACKNOWLEDGMENTS

The work is supported primarily by Indo-U.S. Joint Center for Rational Control of Functional Oxides under Indo-U.S. Science and Technology Forum. Work at the Advanced Photon Source, Argonne was supported by the U.S. Department of Energy, Office of Science under Grant No. DEAC02-06CH11357. S.P. and S.G. acknowledge CSIR for student fellowship. D.D.S. thanks Jamsetji Tata Trust for support.

[1] N. Rogado, J. Li, A. Sleight, and M. Subramanian, Adv. Mater. **17**, 2225 (2005).
[2] M. Hashisaka, D. Kan, A. Masuno, M. Takano, Y. Shimakawa, T. Terashima, and K. Mibu, Appl. Phys. Lett. **89**, 032504 (2006).
[3] S. Zhou, L. Shi, H. Yang, and J. Zhao, Appl. Phys. Lett. **91**, 172505 (2007).
[4] P. Padhan, H. Z. Guo, P. LeClair, and A. Gupta, Appl. Phys. Lett. **92**, 022909 (2008).
[5] M. Kitamura, I. Ohkubo, M. Matsunami, K. Horiba, H. Kumigashira, Y. Matsumoto, H. Koinuma, and M. Oshima, Appl. Phys. Lett. **94**, 262503 (2009).
[6] S. M. Zhou, Y. Q. Guo, J. Y. Zhao, S. Y. Zhao, and L. Shi, Appl. Phys. Lett. **96**, 262507 (2010).
[7] M. Zhu, Y. Lin, E. W. C. Lo, Q. Wang, Z. Zhao, and W. Xie, Appl. Phys. Lett. **100**, 062406 (2012).
[8] D. Choudhury, P. Mandal, R. Mathieu, A. Hazarika, S. Rajan, A. Sundaresan, U. V. Waghmare, R. Knut, O. Karis, P. Nordblad, and D. D. Sarma, Phys. Rev. Lett. **108**, 127201 (2012).
[9] Y. Guo, L. Shi, S. Zhou, J. Zhao, and W. Liu, Appl. Phys. Lett. **102**, 222401 (2013).
[10] D. Chakraborty, U. N. Nandi, D. Jana, M. G. Masud, and S. Giri, J. Appl. Phys. **118**, 035103 (2015).
[11] P. Kumar, S. Ghara, B. Rajeswaran, D. Muthu, A. Sundaresan, and A. Sood, Solid State Commun. **184**, 47 (2014).
[12] M. P. Singh, C. Grygiel, W. C. Sheets, P. Boullay, M. Hervieu, W. Prellier, B. Mercey, C. Simon, and B. Raveau, Appl. Phys. Lett. **91**, 012503 (2007).
[13] X. Wang, Y. Sui, Y. Li, L. Li, X. Zhang, Y. Wang, Z. Liu, W. Su, and J. Tang, Appl. Phys. Lett. **95**, 252502 (2009).
[14] S. Zhao, L. Shi, S. Zhou, J. Zhao, H. Yang, and Y. Guo, J. Appl. Phys. **106**, 123901 (2009).
[15] H. Z. Guo, J. Burgess, E. Ada, S. Street, A. Gupta, M. N. Iliev, A. J. Kellock, C. Magen, M. Varela, and S. J. Pennycook, Phys. Rev. B **77**, 174423 (2008).
[16] H. Guo, A. Gupta, M. Varela, S. Pennycook, and J. Zhang, Phys. Rev. B **79**, 172402 (2009).
[17] Y. Mao, J. Parsons, and J. S. McCloy, Nanoscale **5**, 4720 (2013).
[18] R. Takahashi, I. Ohkubo, K. Yamauchi, M. Kitamura, Y. Sakurai, M. Oshima, T. Oguchi, Y. Cho, and M. Lippmaa, Phys. Rev. B **91**, 134107 (2015).
[19] M. Ullah, S. A. Khan, G. Murtaza, R. Khenata, N. Ullah, and S. B. Omran, J. Magn. Magn. Mater. **377**, 197 (2015).
[20] V. L. J. Joly, P. A. Joy, S. K. Date, and C. S. Gopinath, Phys. Rev. B **65**, 184416 (2002).
[21] C. L. Bull, D. Gleeson, and K. S. Knight, J. Phys.: Condens. Matter **15**, 4927 (2003).
[22] M. N. Iliev, M. M. Gospodinov, M. P. Singh, J. Meen, K. D. Truong, P. Fournier, and S. Jandl, J. Appl. Phys. **106**, 023515 (2009).
[23] M. P. Singh, K. D. Truong, S. Jandl, and P. Fournier, Phys. Rev. B **79**, 224421 (2009).
[24] J. B. Goodenough, A. Wold, R. J. Arnott, and N. Menyuk, Phys. Rev. **124**, 373 (1961).
[25] G. Blasse, J. Phys. Chem. Solids **26**, 1969 (1965).
[26] M. C. Sánchez, J. García, J. Blasco, G. Subías, and J. Perez-Cacho, Phys. Rev. B **65**, 144409 (2002).
[27] R. I. Dass, J.-Q. Yan, and J. B. Goodenough, Phys. Rev. B **68**, 064415 (2003).
[28] K. Asai, H. Sekizawa, and S. Iida, J. Phys. Soc. Jpn. **47**, 1054 (1979).
[29] M. Sonobe and K. Asai, J. Phys. Soc. Jpn. **61**, 4193 (1992).
[30] J. Blasco, M. Sánchez, J. Pérez-Cacho, J. García, G. Subías, and J. Campo, J. Phys. Chem. Solids **63**, 781 (2002).
[31] H. Das, U. V. Waghmare, T. Saha-Dasgupta, and D. D. Sarma, Phys. Rev. Lett. **100**, 186402 (2008).
[32] J. Rodríguez-Carvajal, Physica B (Amsterdam) **192**, 55 (1993).
[33] I. A. Kowalik, G. Öhrwall, B. N. Jensen, R. Sankari, E. Wallén, U. Johansson, O. Karis, and D. Arvanitis, J. Phys.: Conf. Ser. **211**, 012030 (2010).
[34] C. Mitra, Z. Hu, P. Raychaudhuri, S. Wirth, S. I. Csiszar, H. H. Hsieh, H.-J. Lin, C. T. Chen, and L. H. Tjeng, Phys. Rev. B **67**, 092404 (2003).
[35] S. Ray, A. Kumar, D. D. Sarma, R. Cimino, S. Turchini, S. Zennaro, and N. Zema, Phys. Rev. Lett. **87**, 097204 (2001).
[36] F. Nolting, A. Scholl, J. Stohr, J. W. Seo, J. Fompeyrine, H. Siegwart, J.-P. Locquet, S. Anders, J. Luning, E. E. Fullerton, M. F. Toney, M. R. Scheinfein, and H. A. Padmore, Nature (London) **405**, 767 (2000).
[37] K. Horiba, H. Kawanaka, Y. Aiura, T. Saitoh, C. Satoh, Y. Kikuchi, M. Yokoyama, Y. Nishihara, R. Eguchi, Y. Senba, H. Ohashi, Y. Kitajima, and S. Shin, Phys. Rev. B **81**, 245127 (2010).
[38] G. van der Laan and A. I. Figueroa, Coord. Chem. Rev. **277**, 95 (2014).
[39] D. Topwal, U. Manju, S. Ray, S. Raj, D. D. Sarma, S. R. Krishnakumar, M. Bertolo, S. La Rosa, and G. Cautero, J. Chem. Sci. **118**, 87 (2006).
[40] C. Shi, Y. Hao, and Z. Hu, J. Phys. D **44**, 245405 (2011).
[41] W. Z. Yang, X. Q. Liu, H. J. Zhao, Y. Q. Lin, and X. M. Chen, J. Appl. Phys. **112**, 064104 (2012).
[42] J.-S. Kang, S. M. Lee, D. H. Kim, S. Kolesnik, B. Dabrowski, B.-G. Park, J.-Y. Kim, J. Lee, B. Kim, and B. I. Min, J. Appl. Phys. **107**, 09D721 (2010).
[43] J. C. Rojas Sánchez, B. Nelson-Cheeseman, M. Granada, E. Arenholz, and L. B. Steren, Phys. Rev. B **85**, 094427 (2012).
[44] J. Hoffman, I. C. Tung, B. B. Nelson-Cheeseman, M. Liu, J. W. Freeland, and A. Bhattacharya, Phys. Rev. B **88**, 144411 (2013).
[45] B. T. Thole, P. Carra, F. Sette, and G. van der Laan, Phys. Rev. Lett. **68**, 1943 (1992).

Correction: Error values in Table I have been reformatted.